

Results on Jet Spectra and Structure from ALICE

Andreas Morsch (for the ALICE Collaboration)¹

CERN, 1211 Geneva 23, Switzerland

Abstract

Full jet reconstruction in ALICE uses the combined information from charged and neutral particles. Essentially all jet constituents can be measured with large efficiency down to very low transverse momenta ($p_T > 150 \text{ MeV}/c$). This has the advantage to introduce a minimum bias on the jet fragmentation, in particular for low jet momenta and in the presence of quenching. In this article, we present preliminary results from reconstruction of charged jets in Pb–Pb collisions at $\sqrt{s_{\text{NN}}} = 2.76 \text{ TeV}$. The inclusive charged jet spectrum, the jet nuclear modification factors (R_{AA} , R_{CP}), the ratio of spectra measured with different resolution parameters and hadron-jet correlations are discussed. For pp data at the same center of mass energy, the inclusive spectrum of fully reconstructed jets and its resolution parameter dependence are reported.

1. Introduction

The analysis of hadronic jets in heavy-ion collisions represents a formidable tool to study the properties of the Quark-Gluon Plasma. Jets emerge from high- p_T quarks and gluons produced in hard scatterings during the very early phase of the reaction. The partons traverse the medium losing energy through elastic scattering and gluon radiation, a process in general called jet quenching [1]. Comparing heavy ion collisions to more elementary collisions like pp the prominent experimentally observable effects of jet quenching are the decrease of the jet yield, energy imbalance of di-jet events, and the modification of the fragmentation function and the angular distribution of energy with respect to the jet axis.

At the LHC, rates are high at transverse energies where jets can be reconstructed above the fluctuations of the background energy contribution from the underlying event. In particular, for jet transverse energies $E_T > 100 \text{ GeV}$ the influence of the underlying event is relatively small allowing for robust jet measurements [2, 3]. However, the measurements of the suppression of single particle production R_{AA} show that quenching effects are strongest for intermediate transverse momenta ($R_{\text{AA}} < 0.2$ for $4 < p_T < 20 \text{ GeV}/c$ corresponding to parton p_T in the range $\approx 6 - 30 \text{ GeV}/c$) [4]. The objective of ALICE is to access this p_T region introducing the smallest possible bias on the jet fragmentation by measuring jet fragments down to low p_T ($> 150 \text{ MeV}/c$). The key elements of this analysis are the detailed measurement of the underlying event fluctuations (published in Ref. [5]), the development of robust deconvolution procedures for spectra measured with low constituent p_T cuts [6] and the suppression of fake jets (random combination of uncorrelated particles) at low p_T [7].

¹A list of members of the ALICE Collaboration and acknowledgements can be found at the end of this issue.

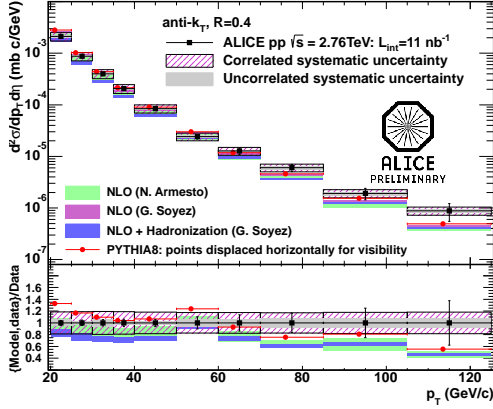


Figure 1: Differential cross section of fully reconstructed jets in pp collisions at $\sqrt{s} = 2.76$ TeV compared to NLO pQCD [11, 12] and PYTHIA8 [13].

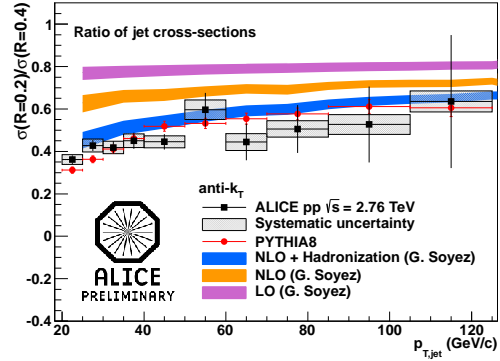


Figure 2: Ratio of jet cross sections reconstructed with $R = 0.2$ and $R = 0.4$ in pp collisions at $\sqrt{s} = 2.76$ TeV compared NLO pQCD [11, 12] and PYTHIA8 [13].

2. Jet Reconstruction in ALICE

In ALICE, full jet reconstruction uses the combined information from charged and neutral particle measurements. Charged particle momentum vectors are measured with the central tracking detectors, the Time Projection Chamber (TPC) and the Inner Tracking System (ITS) covering the full azimuth and $|\eta| < 0.9$. Energy and direction of neutral particles are measured with the Pb-scintillator sampling ElectroMagnetic Calorimeter (EMCal), covering 1/3 of the azimuth and $|\eta| < 0.7$. A detailed description of the ALICE experiment is given in Ref. [8].

For jet reconstruction the anti- k_T algorithm from the FastJet package [9] with resolution parameters R varying between 0.2 and 0.4 is used. The jet 4-momentum vector is calculated using the boost invariant p_T recombination scheme. Analysis with charged jets using only tracking information and fully reconstructed jets including EMCal information have been performed. The input for charged jets are tracks with $p_T > 150$ MeV/c. The input for fully reconstructed jets is the charged jet input adding the EMCal cluster energy with E_T above 150 MeV/c after correcting for charged particle energy contributions. These jets are required to be fully contained in the EMCal acceptance.

Jet-by-jet we correct for the energy contribution from charged particles to the energy measured with EMCal and the contribution from the underlying event. The sum of momenta of charged tracks matching the EMCal clusters from the cluster energy is subtracted resetting negative values to zero:

$$E_{\text{clus}}^{\text{corr}} = E_{\text{clus}}^{\text{raw}} - c \cdot \sum p^{\text{matched}}; E_{\text{clus}}^{\text{corr}} > 0 \quad (1)$$

The nominal value of c is unity and is varied over a wide range to estimate the systematic uncertainty of this procedure.

In Pb–Pb collisions, one has also to subtract the contribution of the Underlying Event (UE) from the reconstructed jet p_T . The summed p_T from the background is calculated as the product of mean momentum density ρ and the jet area A^{jet} , where ρ is determined using the k_T -algorithm [10] via: $\rho = \text{median}(\frac{p_T^{\text{jet}}}{A^{\text{jet}}})$. Further corrections can only be applied on the raw spectrum bin-by-bin or using unfolding techniques. These corrections comprise the unmeasured p_T from neutrons

and K_L^0 , as well as the tracking efficiency and the corresponding jet-by-jet fluctuations of these quantities. In Pb–Pb collisions, we also correct for the smearing of the spectra induced by the UE energy fluctuations. This smearing is quantified by δp_T , the difference between the UE corrected summed p_T and the true jet p_T : $\delta p_T = (p_T^{\text{rec}} - \rho A^{\text{jet}}) - p_T^{\text{true}}$.

A data-driven method to determine the distribution of δp_T consists of embedding different objects into measured Pb–Pb collisions [5]. These objects can be single high- p_T tracks, jets or random cones. An advantage of the anti- k_T algorithm is, that the distribution does not depend significantly on the embedded object. The distribution is almost Gaussian with enhanced tails towards positive differences, owing to the pile-up of jets in the same jet area. For a resolution parameter $R = 0.2$ the width (σ) of the Gaussian amounts to 6.2 GeV/c (4.5 GeV/c) summing neutral and charged p_T (for charged particles only).

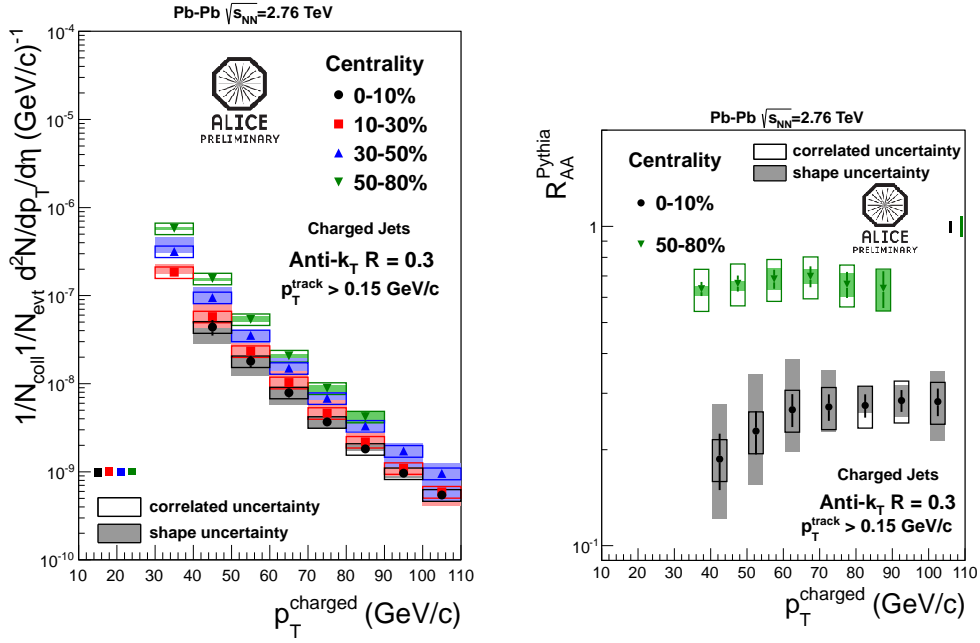


Figure 3: Left: Corrected jet spectrum with charged tracks for jet radius $R = 0.3$. Right: Nuclear modification factor for charged jets reconstructed in central and peripheral Pb–Pb collisions. The pp reference is obtained from PYTHIA simulation at the same \sqrt{s} .

3. Jet Spectra in pp at $\sqrt{s} = 2.76$ TeV

In March 2011, a short pp reference run at the Pb–Pb energy of 2.76 TeV was taken integrating 20 nb^{-1} of rare triggers. This was the first running period in which the EMCAL was fully installed allowing us to perform measurements with fully reconstructed jets up to 120 GeV/c from 11 nb^{-1} of these data. Fig. 1 shows the jet p_T spectrum reconstructed with a resolution parameter of $R = 0.4$. The jet energy scale uncertainty amounts to 4% and it is mainly due to uncertainties in the missing neutral energy, the tracking efficiency and energy double-counting.

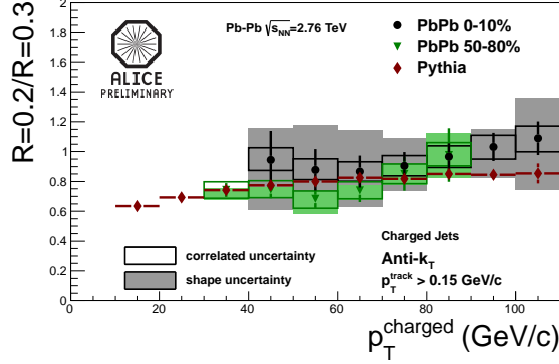


Figure 4: Ratio of reconstructed charged jets with different cone radii in central and peripheral Pb–Pb collisions at $\sqrt{s_{NN}} = 2.76$ TeV compared to PYTHIA (unquenched).

The jet p_T resolution $\Delta p_T/p_T$ amounts to 20% and is dominated by the jet energy scale fluctuations, tracking and EMCal resolutions. Efficiency and resolution effects on the jet spectrum were taken into account by applying a bin-by-bin correction. The measured spectrum is compared to NLO pQCD calculations [11, 12] and PYTHIA8 [13]. A good agreement is observed. The measurement itself represents an important reference for our Pb–Pb measurements.

Ratios of differential cross-sections measured with different R provide information on the energy distribution within the jet area (jet shape). Note that for jets reconstructed with the anti- k_T algorithm, R is to a good approximation the radius of a circular jet area. Fig. 2 shows the measured ratio for $R = 0.2$ and 0.4 . Due to the fact that higher p_T jets are more collimated, the ratio rises with p_T^{Jet} ; in agreement with the pQCD and PYTHIA8 calculations.

4. Jet Suppression in Pb–Pb

Measurements of jet spectra in Pb–Pb collisions were obtained from a sample of $3 \cdot 10^7$ minimum bias events at $\sqrt{s_{NN}} = 2.76$ TeV collected in November 2010. Since the electromagnetic calorimeter was only fully installed in the beginning of 2011, jet reconstruction was performed using charged particle information only.

Fig. 3 (left) shows the charged jet yields as a function of p_T normalized by the number of collisions (resolution parameters $R = 0.3$) for four centrality classes. The influence of detector effects and background fluctuations were corrected for by applying a regularized unfolding procedure with χ^2 minimization. The systematic uncertainties are dominated by the choice of the unfolding parameters (4%) and the jet energy scale corrections (4 – 10%).

Comparing the spectra for different centrality classes a sizable suppression increasing with centrality can be observed. In order to study the modifications of the Pb–Pb spectra with respect to an incoherent superposition of binary nucleon–nucleon collisions, the nuclear modification factor R_{AA}^{Jet} was calculated and is shown in Fig. 3 (right). As a reference we use the spectra from pp collisions at the same centre-of-mass energy simulated by the PYTHIA MC [13]. The results for the highest centrality bin (0-10%) and the lowest one (50-80%) for $R = 0.2$ are shown. A strong nuclear suppression qualitatively and quantitatively similar to the R_{AA} of inclusive hadrons is observed in the most central collisions.

A possible effect of jet quenching is the redistribution of the radiated energy within the jet cone leading to jet shape modifications. As mentioned earlier the ratios of differential cross-sections measured with different R can provide information on these jet shape modifications. Fig. 4 shows the measured ratio $(R = 0.2)/(R = 0.3)$. No modifications of the jets measured in central Pb–Pb collisions with respect to more peripheral collisions or the PYTHIA pp reference are observed within the present large experimental uncertainties.

The requirement of a high p_T leading hadron within the jet area reduces the contribution from combinatorial (fake) jets. This leads to an improved stability of the unfolding and allows us to assess lower $p_{T,\text{Jet}}^{\text{ch}}$. Using a resolution parameter $R = 0.2$ we can measure the charged jet spectrum down to 20 GeV/c. In Fig. 5 (left) we compare the inclusive spectrum to those with $p_T^{\text{leading}} > 5$ GeV/c and $p_T^{\text{leading}} > 10$ GeV/c requirement. For central collisions (0-10%), we observe no change of fragmentation within uncertainties except for the lowest $p_{T,\text{Jet}}^{\text{ch}}$ bin. To quantify the jet suppression in central collisions we plot in Fig. 5 (right) the ratio of the jet yield with respect to centrality 50 – 80% (R_{CP}). It shows a suppression pattern similar to R_{AA} . For more details see the contribution of M. Verweij to these proceedings.

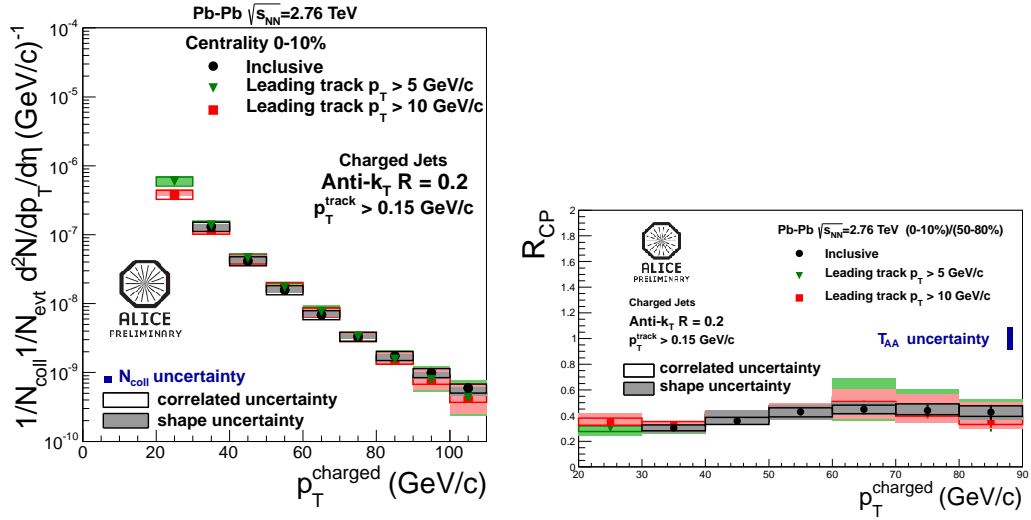


Figure 5: Charged jet measurements in Pb–Pb using the high- p_T hadron tag and resolution parameter $R = 0.2$. Left: Corrected charged jet spectrum for central Pb–Pb collisions. Right: R_{CP} relative to the centrality bin 50 – 80%.

5. Hadron-Jet Correlations

In the presence of strong partonic energy loss, leading hadron emission is biased towards the surface of the reaction zone. Hence, the in-medium path-length of the parton produced back-to-back to the leading particle is above average and the jet emerging from this parton can be expected to show stronger than average suppression and structure modifications [14]. To exploit this effect we study the conditional yield of jets produced opposite in azimuth to a leading particle within a given p_T range $p_T^{\text{min}} - p_T^{\text{max}}$:

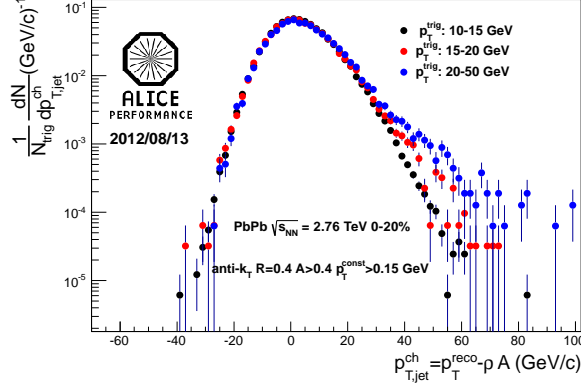


Figure 6: Uncorrected recoil jet yield per trigger differential in p_T for three trigger p_T ranges.

$$Y(p_{T,\text{Jet}}^{\text{ch}}; p_T^{\text{min}}, p_T^{\text{max}}) = \frac{1}{N_{\text{tr}}} \frac{dN(p_{T,\text{Jet}}^{\text{ch}}; p_T^{\text{min}}, p_T^{\text{max}})}{dp_{T,\text{Jet}}^{\text{ch}}} \quad (2)$$

The method has additional advantages. There is no bias on the fragmentation of the recoiling jet. Moreover, the requirement of a correlated high- p_T hadron tags hard scatterings and suppresses the combinatorial, fake jet background at low jet p_T .

Fig. 6 shows the uncorrected recoil charged jet yield per trigger differential in p_T . The azimuthal distance between trigger hadron and jet is required to be in the region $\pi \pm 0.6$. Three trigger p_T bins are shown. The low jet p_T region is almost independent of the trigger p_T and dominated by fake and uncorrelated jets. The high jet p_T region shows a clear hardening with increasing trigger p_T and is dominated by high Q^2 scattering.

The uncorrelated background does not depend on the trigger hadron p_T range. Hence, in the difference between the per trigger yields for two different trigger p_T ranges $\Delta_{\text{recoil}}(p_{T,\text{Jet}}^{\text{ch}})$ the uncorrelated background cancels. We define:

$$\Delta_{\text{recoil}}(p_{T,\text{Jet}}^{\text{ch}}) = Y(p_{T,\text{Jet}}^{\text{ch}}; p_T^{\text{min}}, p_T^{\text{max}}) - Y(p_{T,\text{Jet}}^{\text{ch}}; p_{T,\text{ref}}^{\text{min}}, p_{T,\text{ref}}^{\text{max}}) \quad (3)$$

Modifications of the conditional yields in central Pb–Pb collisions have been studied measuring the ratio

$$\Delta I_{\text{AA}}(p_{T,\text{Jet}}^{\text{ch}}) = \Delta_{\text{recoil}}^{\text{Pb–Pb}} / \Delta_{\text{recoil}}^{\text{pp}} \quad (4)$$

The fully corrected ratios for two different resolution parameters are shown in Fig. 7. A trigger p_T range 20 – 50 GeV/c was used for the signal and 15 – 20 GeV/c for the reference. Again results of a PYTHIA simulation were used as pp reference. The ratio is close to unity close to the conditional away-side hadron-hadron yield suppression measured by ALICE at a lower Q^2 [15]. Note, however, that the hadron-jet pair suppression is strong. It is approximately $R_{\text{AA}}(20 \text{ GeV}/c) \times \Delta I_{\text{AA}} \approx 0.25 \times 0.75 \approx 0.2$. For more details see the contribution of L. Cunqueiro to these proceedings.

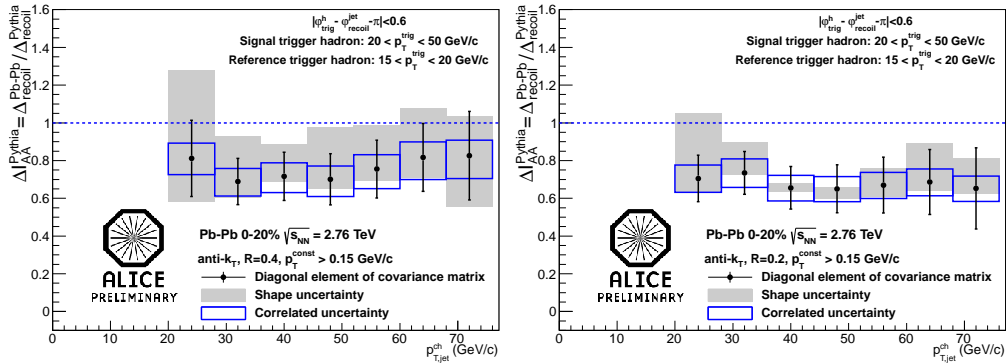


Figure 7: The ratio ΔI_{AA} using PYTHIA as the pp reference for two different resolution parameter: $R = 0.4$ (left) and $R = 0.2$ (right).

6. Isolated Photon-Hadron Correlations in pp

A very attractive possibility for studying jets at lower energy in heavy-ion collisions consists of tagging jets by γ -jet correlations. Direct gammas result in leading order from annihilation and Compton scattering ($q + g(q)\gamma + q(g)$). In contrast to partons, gammas penetrate the medium almost unaltered. They approximately balance the transverse energy of the original parton and, hence, can be used to assess the jet energy. Experimentally one can tag such processes by identifying leading isolated photons and correlated associated charged hadrons in the opposite azimuthal direction. Photons are detected in the EMCal. Photon candidates are reconstructed from clusters of energy deposited in the p_T range from 8 to 25 GeV/c. These candidates are dominated by background from electromagnetic decays of neutral mesons. Since these particles are mainly produced in jets, the background can be reduced by imposing an isolation criteria. In our analysis we require that no particle with $p_T > 0.5$ GeV/c is found within a cone of radius $R = 0.4$.

The fragmentation function of the recoiling jet can be approximated by the x_E distribution, where $x_E = p_T^{hadron} / p_T^\gamma \cos \Delta\varphi$. Fig. 8 shows the measured x_E distribution for $p_T^{hadron} > 0.2$ GeV/c after correction for residual background. The distribution can be fit by an exponential function with inverse slope 7.8 ± 0.9 . The measurement of the x_E distribution and the inverse slope from γ -hadron correlations represents a first important step towards corresponding measurements in Pb-Pb. For more details see the contribution of N. Arbor to these proceedings.

7. Summary

Preliminary measurement in central Pb-Pb collisions at $\sqrt{s_{NN}} = 2.76$ TeV show a strong suppression of the inclusive charged jet yield. Using PYTHIA as a reference, the nuclear suppression factor R_{AA} for charged jets amounts to $0.2 - 0.3$ in the range $30 < p_{T,ch}^{ch} < 100$ GeV/c, lower than the inclusive hadron R_{AA} at similar parton p_T . No indication of energy redistribution within experimental uncertainties is observed from ratios of jet yields ($R = 0.2$)/($R = 0.3$). The conditional hadron-jet yield is suppressed by a factor of 0.75 with respect to the PYTHIA reference. This is close to the conditional away-side hadron-hadron yield suppression measured by ALICE at a lower Q^2 . The yield and conditional yield suppression patterns are qualitatively and to some extent quantitatively similar for single hadrons and jets. This is qualitatively consistent

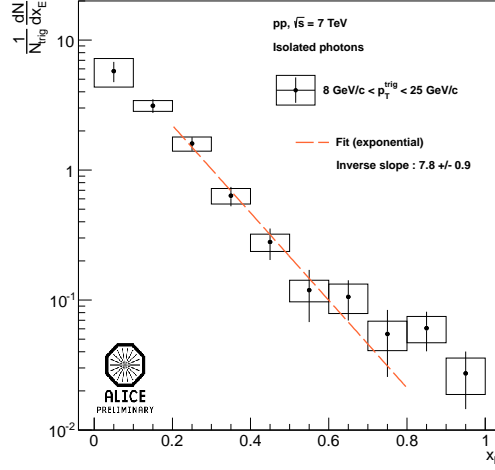


Figure 8: x_E distributions (with : $x_E = -p_T^{\text{asso}}/p_T^{\text{trig}} \cos \Delta\varphi$) of isolated photons for the p_T range $p_T = 8 - 25$ GeV/c. The red line show the result of an exponential fit in the range [0.2-0.8].

with the expectations for partonic energy loss through radiation mainly outside the jet cone and in-vacuum fragmentation of the remnant parton. First preliminary results from γ -hadron correlations measurements and x_E in pp at $\sqrt{s} = 7$ TeV have been presented. They represent an important step towards a corresponding measurement in Pb–Pb.

References

References

- [1] U.A. Wiedemann, *Jet Quenching in Heavy Ion Collisions*, [arXiv:0908.2306].
- [2] G. Aad *et al.* (ATLAS Collaboration), *Phys. Rev. Lett.* **105**, 252303 (2010).
- [3] S. Chatrchyan *et al.* (CMS Collaboration), *Phys. Rev.* **C84**, 024906 (2011).
- [4] K. Aamodth *et al.* (ALICE Collaboration), *Phys. Lett.* **B696** 30-39 (2011).
- [5] B. Abelev *et al.* (ALICE Collaboration), *JHEP* **1203**, 053 (2012).
- [6] M. Verweij, (ALICE Collaboration), *Measurement of jet spectra in Pb-Pb collisions at $\sqrt{s_{NN}}=2.76$ TeV with the ALICE detector at the LHC*, [arXiv:1208.6169].
- [7] G.O.V. de Barros *et al.*, *Data-driven analysis methods for the measurement of reconstructed jets in heavy ion collisions at RHIC and LHC*, [arXiv:1208.1518].
- [8] K. Aamodt *et al.* (ALICE Collaboration), *JINST* **3**, S08002 (2008).
- [9] M. Cacciari, G. P. Salam and G. Soyez, *Eur.Phys.J.* **C72**, 1896 (2012).
- [10] M. Cacciari and G. P. Salam, *Phys. Lett.* **B659**, 119 (2008).
- [11] G. Soyez, *Phys. Lett. B* **698**, 59 (2011) [arXiv:1101.2665v1]; private communication.
- [12] N. Armesto, private communication. Calculations based on:
S. Frixione, Z. Kunszt, and A. Signer, *Nucl. Phys.* **B467**, 399-442 (1996);
S. Frixione, *Nucl. Phys.* **B507**, 295-314 (1997).
- [13] T. Sjöstrand, S. Mrenna and P. Skands, *JHEP* **05**, 026 (2006);
T. Sjostrand, S. Mrenna and P. Z. Skands, *Comput. Phys. Commun.* **178**, 852 (2008).
- [14] T Renk, [arXiv:1204.5572].
- [15] K. Aamodt *et al.* (ALICE Collaboration), *Phys. Rev. Lett.* **108**, 092301 (2012).